# NLRP3 activation in tumor-associated macrophages enhances lung metastasis of pancreatic ductal adenocarcinoma

**Haitao Gu[1#], Wensheng Deng[2#], Yi Zhang[3#], Yu Chang[4], Vishal G. Shelat[5], Kunihiro Tsuchida[6], Leonardo S. Lino-Silva[7], Zhaowen Wang[1]**

[1]Department of General Surgery, Shanghai General Hospital, Shanghai Jiao Tong University School of Medicine, Shanghai, China; [2]Department of General Surgery, Gastrointestinal Surgical Institute, the First Affiliated Hospital of Nanchang University, Nanchang, China; [3]Department of Colorectal Surgery, the First Affiliated Hospital of Nanjing Medical University, Nanjing, China; [4]Department of Endocrinology, the Third People's Hospital of Yunnan, Dali University School of Medicine, Kunming, China; [5]Department of General Surgery, Tan Tock Seng Hospital, Singapore, Singapore; [6]Division for Therapies Against Intractable Diseases, Institute for Comprehensive Medical Science (ICMS), Fujita Health University, Toyoake, Aichi, Japan; [7]Department of Surgical Pathology, Instituto Nacional de Cancerología, Tlalpan, Mexico City, Mexico

*Contributions:* (I) Conception and design: H Gu; (II) Administrative support: H Gu; (III) Provision of study materials or patients: H Gu; (IV) Collection and assembly of data: All authors; (V) Data analysis and interpretation: All authors; (VI) Manuscript writing: All authors; (VII) Final approval of manuscript: All authors.

[#]These authors contributed equally to this work and should be considered as co-first authors.

*Correspondence to:* Zhaowen Wang. Department of General Surgery, Shanghai General Hospital, Shanghai Jiao Tong University School of Medicine, 100 Haining Road, Hongkou District, Shanghai 200080, China. Email: zhaowenw@163.com.

**Background:** Pancreatic ductal adenocarcinoma (PDAC) is the most common type of pancreatic cancer and is highly malignant due to its late diagnosis and early metastasis. Lung metastasis of PDAC occurs in a significant number of diagnosed patients and represents high severity of disease and poor clinical outcome. However, the molecular regulation of lung metastasis of PDAC is still not fully understood. Tumor-associated macrophages (TAMs) have recently been found to play an important role in cancer initiation, proliferation, progression, and metastasis. The proliferation, differentiation, and polarization of macrophages has been shown to be regulated by interleukin 1β (IL-1β), which is generated by NLR family pyrin domain containing 3 (NLRP3)-induced formation of inflammasome. Herein we investigated whether NLRP3 plays a role in lung metastasis of PDAC through regulation of macrophage polarization.

**Methods:** Gene profiles for NLRP3 (+/+) and NLRP3 (–/–) macrophages obtained from the Gene Expression Omnibus (GEO) public database were compared and analyzed for altered genes related to macrophage polarization. The regulation of macrophage polarization by NLRP3 was examined in a coculture system with naïve NLRP3 (+/+) or NLRP3 (–/–) macrophages and PDAC cells. Cell growth was analyzed by a Cell Counting Kit-8 (CCK-8) assay. Cell invasiveness and migratory potential were analyzed by transwell cell invasion assay and cell migration assay, respectively. PDAC formation and lung metastasis were analyzed in a mouse model of PDAC with and without NLRP3 knockout.

**Results:** GEO database analysis revealed significant alteration in genes that regulate macrophage polarization in NLRP3-depleted macrophages. NLRP3-depletion in macrophages seemed to favor an M1/M2b polarization. *In vitro*, the presence of NLRP3 in macrophages led to M2a/c/d TAM-like polarization when they were cocultured with PDAC cells. Conversely, NLRP3 depletion in macrophages led to M1/M2b polarization when they were cocultured with PDAC cells. NLRP3-depletion significantly inhibited tumor growth and stage progression in a mouse model of PDAC and significantly reduced the occurrence of lung metastasis.

**Conclusions:** Our results suggested that NLRP3 activation in TAM enhanced lung metastasis of PDAC through regulation of TAM polarization.

**Keywords:** Pancreatic ductal adenocarcinoma (PDAC); lung metastasis; tumor-associated macrophages (TAMs); NLR family pyrin domain containing 3 (NLRP3); macrophage polarization

## Introduction

Pancreatic ductal adenocarcinoma (PDAC) is the most common type of pancreatic cancer and is a biologically aggressive malignancy due to its late diagnosis and early metastasis (1). Tumor metastasis contributes to cancer associated mortality risk (2). Lung metastasis of PDAC occurs in a significant number of patients and represents the high severity of the disease and is associated with poor clinical outcome (3).

The molecular regulation of lung metastasis of PDAC has been extensively studied, showing the importance of the interaction between PDAC cells and their altered microenvironment (4). Among the cells of the tumor microenvironment (TME), tumor-associated macrophages (TAMs) play a pivotal role in the creation of an immunosuppressive TME through production and secretion of a number of cytokines, chemokines, and growth factors to facilitate tumor progression and metastasis (5-7). Macrophages can display in either a classical proinflammatory phenotype ("M1" macrophages), or in an anti-inflammatory phenotype ("M2" macrophages). The alteration of macrophage phenotype to carry certain M1 or M2 characteristics is termed "polarization" (8). TAMs are polarized from naïve macrophages and appear more M2-like (anti-inflammatory). M2 macrophages have 4 major subtypes, named M2a, M2b, M2c, and M2d. M2a polarization is induced by interleukin 4 (IL-4) or IL-13, leading to enhancement of the endocytic activity of macrophages to promote cell growth and tissue repair (8). M2b polarization is activated by immune complexes and regulates the extension of immune reactions (8). M2c polarization is induced by glucocorticoids, transforming growth factor beta 1 (TGFβ1) and IL-10, and appears critical for tissue remodeling (8). M2d macrophages release vascular endothelial growth factor (VEGF) and promote angiogenesis (8). In general, TAMs have characteristics of M2a, M2c, and M2d, while M2b is closer to M1 (8).

The molecular activation of TAMs in PDAC has not been fully determined. IL-1β, a proinflammatory cytokine, plays a vital role in tumor progression and metastasis (9). A recent study has shown that activation of IL-1β in cells usually requires the involvement of a protein complex called inflammasome (10). The inflammasome is formed by NOD-like receptors (NLRs) to participate in the process of dimerization of caspase-1, leading to its activation, which subsequently turns the IL-1β precursor (pro-IL-1β) into its activated form, IL-1β, for secretion (11). However, it is not known whether NLR family pyrin domain containing 3 (NLRP3) plays a role in lung metastasis of PDAC through regulation of macrophage polarization.

In this study, we aimed to use database analysis and a set of *in vitro* and *in vivo* experiments to determine the effects of NLRP3 activation in TAMs on lung metastasis of PDAC. We present the following article in accordance with the ARRIVE reporting checklist (available at https://tlcr.amegroups.com/article/view/10.21037/tlcr-22-311/rc).

## Methods

### Experimental approval

The present study was approved by the Research and Animal Ethics Association of the Shanghai Jiao Tong University School of Medicine (No. 2014KY038) in compliance with Shanghai Jiao Tong University School of Medicine guidelines for the care and use of animals. A protocol was prepared before the study without registration. No criteria were used for excluding any experimental units during the experiment, and no data were excluded during the analysis. The study did not involve human specimens.

### Animals

The role of NLRP3 in PDAC was examined in P48[Cre]; LSL-KrasG12D (KC) mice model (Jax Mice, Carlsbad, CA, USA), which express oncogenic Kras in pancreatic progenitor cells (12). KC mice were bred with NLRP3-deficient mice (B6.129S6-Nlrp3tm1Bhk/J, Jax Mice) to obtain KC NLRP3 (–/–) mice (– represents depletion of the gene). The KC NLRP3 (+/+) mice (+ represents wildtype gene without any depletions) were used as controls. Mice were housed in a standardized environment with good ventilation, light/dark cycle (12:12 hours), quiet and regular animal husbandry.

### PDAC cell lines and macrophages

Human PDAC cell lines PANC-1 and SW1990 were

both purchased from American Type Culture Collection (Rockville, MD, USA). PANC-1 and SW1990 cells were cultured in Dulbecco's Modified Eagle's Medium (DMEM; Invitrogen, Carlsbad, CA, USA) supplemented with 8% fetal bovine serum (FBS; Sigma-Aldrich, St Louis, MO, USA) in a humidified chamber with 5% $CO_2$ at 37 ℃. Mouse bone marrow was obtained and resuspended in DMEM to form a mononuclear white layer in 6-well plates ($2\times10^6$ cells/mL, 3.5 mL/well; Falcon, Corning, NY, USA). After 2 hours, cells were washed 2 times and adherent cells (monocytes) were kept culturing in DMEM with 10% heat-inactivated FBS supplemented with 20 ng/mL macrophage colony-stimulating factor (M-CSF) for 7–9 days. Half of the medium was refreshed every 2–3 days. The purity of adherent cells after 3 days was analyzed using a multicolor panel of primary monoclonal antibodies against CD3, CD86, and CD11b. For macrophage differentiation, M1 was induced by 20 ng/mL M-CSF and 30 ng/mL lipopolysaccharides (LPS); M2a was induced by 20 ng/mL M-CSF and 20 ng/mL IL-4; M2b was induced by 20 ng/mL M-CSF, 20 ng/mL LPS, and 50 μg/mL immune complex; M2c was induced by 20 ng/mL M-CSF, 20 ng/mL IL-10, and 20 ng/mL TGFβ1; and M2d was induced by 20 ng/mL M-CSF, 20 ng/mL IL-6, and 20 ng/mL toll-like receptor (TLR) ligands.

### Tissue histology and immunohistochemistry

At the time of mouse sacrifice (6 months of age), $CO_2$ inhalation was used as the euthanasia method. Mouse pancreatic or lung specimens were fixed with 10% buffered formalin, dehydrated in 70% ethanol, followed by paraffin embedding, and staining with hematoxylin and eosin (H&E). Immunohistochemistry for NLRP3 was performed with a rabbit polyclonal anti-NLRP3 antibody (1:500; no antigen retrieval; 768319; R&D Systems, Waltham, MA, USA) with Dolichos biflorus agglutinin (DBA). The images were taken from an Olympus Microscopy Photographing System. Pancreatic ductal dysplasia was evaluated based on established criteria (13). Lung metastasis was determined by H&E staining based on section analysis at 100 μm intervals from the serial sectioning of the whole lung.

### RNA extraction and quantitative real-time polymerase chain reaction (RT-qPCR)

Total RNA was extracted using a RNeasy kit (Qiagen, Shanghai, China). Complementary DNA (cDNA) was generated using a reverse transcription kit (Qiagen). RT-qPCR was performed with the SYBR Green PCR Kit (Qiagen) and primers (Qiagen). Duplicated reactions were performed for RT-qPCR to reduce variation. The $2^{-\Delta\Delta Ct}$ method was used to quantify expression of genes of interest. Glyceraldehyde-3-phosphate dehydrogenase (GAPDH) was used as house-keeping gene.

### Enzyme-linked immunosorbent assay (ELISA)

A radioimmunoprecipitation assay (RIPA) buffer (Sigma-Aldrich) was used to extract protein and the bicinchoninic acid assay (BCA) protein assay (Sigma-Aldrich) was used to measure protein concentration. ELISA was performed using ELISA kits for IL-4, IL-6, IL-10, inducible nitric oxide synthase (iNOS), arginase (ARG1), tumor necrosis factor alpha (TNFα), TGFβ1, and VEGF-A (all from R&D Systems).

### Cell proliferation assay

Cell Counting Kit-8 (CCK-8, Sigma-Aldrich) was used to assess cell proliferation. Wells were run in duplicate.

### Cell invasion and migration assay

In the cell invasion assay, 24-well plates (Millipore, Bedford, MA, USA) were precoated with Matrigel (Sigma-Aldrich), then the upper chamber was seeded with cells, and the lower chamber was filled with DMEM with 8% FBS. After 24 hours, cells invaded to the lower chamber were stained with 0.1% crystal violet (Sigma-Aldrich) for 15 minutes before quantification. For cell migration assay, cells in serum-free DMEM were seeded in the upper chamber of a 24-well transwell plate (Millipore), and DMEM with 8% FBS was put in the lower chamber. After 36 hours, cells that had migrated from the upper chamber to the lower surface were fixed with methanol and stained with 0.1% crystal violet (Sigma-Aldrich) for quantification.

### Statistical analysis

Power test was used to determine the number of mice used in experiments. Data were statistically analyzed with GraphPad Prism 7 (GraphPad, Chicago, IL, USA) using one-way analysis of variance (ANOVA) with a Bonferroni correction. Data are presented as mean ± standard deviation (SD). $P<0.05$ was considered statistically significant.
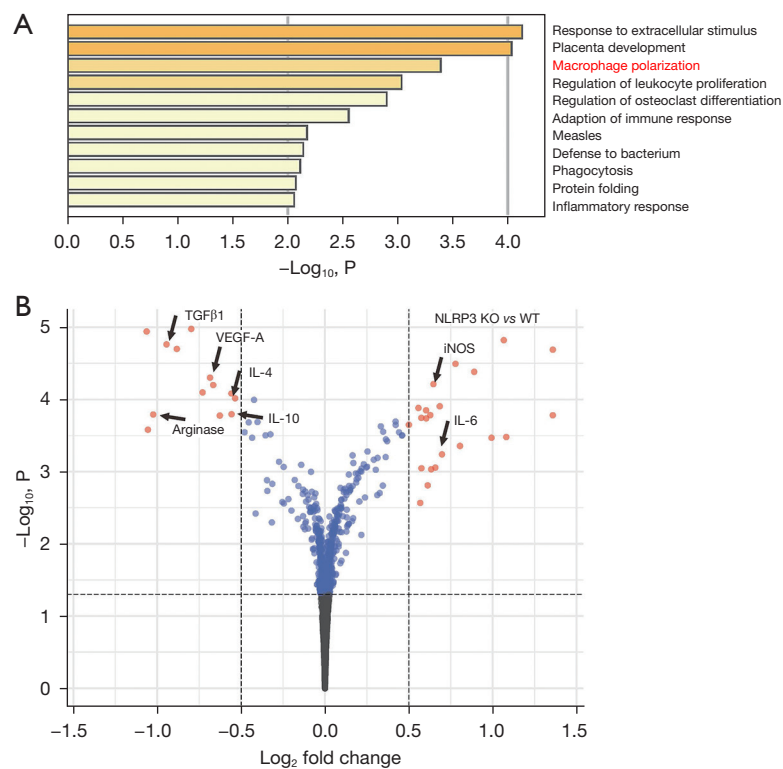
**Figure 1** GEO database shows that macrophage polarization is significantly altered by NLRP3 depletion. (A,B) Gene profiles of NLRP3 (+/+) and NLRP3 (–/–) macrophages obtained from the GEO database (GSE183698) were compared and analyzed for the altered genes related to macrophage polarization. (A) A pathway enrichment analysis was performed using Metascape, showing that many pathways that were greatly altered were associated with inflammation and macrophage polarization (in red). (B) Significantly altered genes shown in a volcano map, with those associated with macrophage polarization highlighted. TGFβ1, transforming growth factor beta 1; VEGF-A, vascular endothelial growth factor A; IL, interleukin; NLRP3, NLR family pyrin domain containing 3; KO, knockout; WT, wildtype; iNOS, inducible nitric oxide synthase; GEO, Gene Expression Omnibus.

RNA-sequencing (RNA-seq) data on mouse macrophages with or without NLRP3 depletion were obtained from the Gene Expression Omnibus (GEO) database (GSE183698; https://www.ncbi.nlm.nih.gov/geo/). The data were analyzed with linear models for microarray and RNA-seq data (Limma) package in R software. Cuffdiff was applied for assessing pairwise differential expression. Log2 |fold change| >1 and a false discovery rate (FDR) <0.05 were used as the cutoff values.

## Results

### GEO database shows that macrophage polarization is significantly altered by NLRP3 depletion

Gene profiles for NLRP3 (+/+) and NLRP3 (–/–) macrophages obtained from the GEO database

(GSE183698) were compared and analyzed for altered genes related to macrophage polarization. The signaling pathways that were substantially altered included many associated with inflammation and most importantly, macrophage polarization (*Figure 1A*). As shown in the volcano map, we detected significant alteration in genes that regulate macrophage polarization in NLRP3-depleted macrophages, including downregulation of ARG1, IL-4, IL-10, TGFβ1, and VEGF-A, and upregulation of IL-6 and iNOS (*Figure 1B*). ARG1 is an M2 marker, IL-4 is predominantly expressed by M2a, IL-10 is predominantly expressed by M2c and M2d, TGFβ1 is predominantly expressed by M2c, and VEGF-A is predominantly expressed by M2c, while iNOS and IL-6 are predominantly expressed by M1 and M2b. These data suggested that NLRP3-depletion in macrophages seemed to favor a polarization
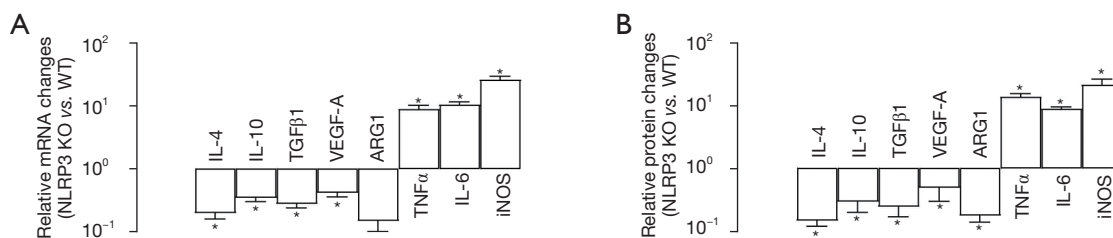
**Figure 2** NLRP3-depleted macrophages turn proinflammatory. Peritoneal macrophages were isolated from NLRP3-knockout mice and wildtype control mice. (A,B) RT-qPCR (A) and ELISA (B) were performed to analyze levels of factors associated with macrophage polarization. *, P<0.05. N=5. NLRP3, NLR family pyrin domain containing 3; KO, knockout; WT, wildtype; IL, interleukin; TGFβ1, transforming growth factor beta 1; VEGF-A, vascular endothelial growth factor A; ARG1, arginase 1; TNFα, tumor necrosis factor alpha; iNOS, inducible nitric oxide synthase; RT-qPCR, real-time polymerase chain reaction; ELISA, enzyme-linked immunosorbent assay.

from M2a/c/d to M1/M2b. In other words, macrophages are likely polarized towards proinflammatory phenotypes by NLRP3 depletion.

### NLRP3-depleted macrophages turn proinflammatory

To confirm the GEO database findings, we isolated peritoneal macrophages from NLRP3-knockout (KO) mice and compared those from control wildtype mice. The factors associated with macrophage polarization were analyzed by RT-qPCR (*Figure 2A*) and ELISA (*Figure 2B*), which showed significant downregulation of ARG1, IL-4, IL-10, TGFβ1, and VEGF-A, and significant upregulation of TNFα, IL-6, and iNOS. These data thus confirmed the findings from the GEO database, suggesting that NLRP3-depletion in macrophages seemed to favor a polarization from M2a/c/d to M1/M2b. In other words, macrophages are likely polarized towards proinflammatory phenotypes by NLRP3 depletion. This could be important since TAMs are mostly like M2d, still close to M2a and M2c. The M1/M2b polarization of macrophages should decrease their potential to promote tumor growth and metastasis.

### NLRP3-depletion in macrophages decreases the cell growth, invasion, and migration of cocultured PDAC cells

The regulation of macrophage polarization by NLRP3 was then examined in a coculture system with naïve NLRP3 (+/+) or NLRP3 (–/–) macrophages and PDAC cells. Cell growth was analyzed by CCK-8 assay. We found that the presence of macrophages at coculture significantly increased the number of viable PANC-1 (*Figure 3A*) or SW1990 cells (*Figure 3B*), and this increase was significantly attenuated by NLRP3-depletion in macrophages (*Figure 3B*). Cell

invasiveness and migratory potential were then analyzed by transwell cell invasion assay and cell migration assay, respectively. We found that the presence of macrophages at coculture significantly increased the invasiveness of PANC-1 or SW1990 cells (*Figure 3C,3D*), and this increase was significantly attenuated by NLRP3-depletion in cocultured macrophages (*Figure 3C,3D*). Moreover, the presence of macrophages at coculture significantly increased the migratory potential of PANC-1 or SW1990 cells (*Figure 3E,3F*), and the increase in migratory potential of PDAC cells was significantly attenuated by NLRP3-depletion in cocultured macrophages (*Figure 3E,3F*). Together, these data suggested that NLRP3-depletion in macrophages decreased cell growth, invasion, and migration of cocultured PDAC cells.

### Differentiation of M1, M2a, M2b, M2c, and M2d macrophages

Since NLRP3 depletion in macrophages altered cocultured PDAC cell growth, invasiveness, and migratory potential and likely altered the macrophage polarization towards proinflammatory phenotypes, we aimed to determine whether the effects on PDAC cells of depletion of NLRP3 in macrophages were through macrophage polarization. Thus, naïve macrophages were differentiated into M1, M2a, M2b, M2c, and M2d macrophages by established methods, and the expression of polarization markers was analyzed by RT-qPCR (*Figure 4A*) and ELISA (*Figure 4B*). We found that the highest level of iNOS was detected in M1, and levels of iNOS in M2b were significantly higher than in M2a, M2c, and M2d (*Figure 4A,4B*). Similar findings were detected in IL-6 (*Figure 4A,4B*). Meanwhile, levels of ARG1 and IL-4 were significantly lower in M2b compared to M2a,
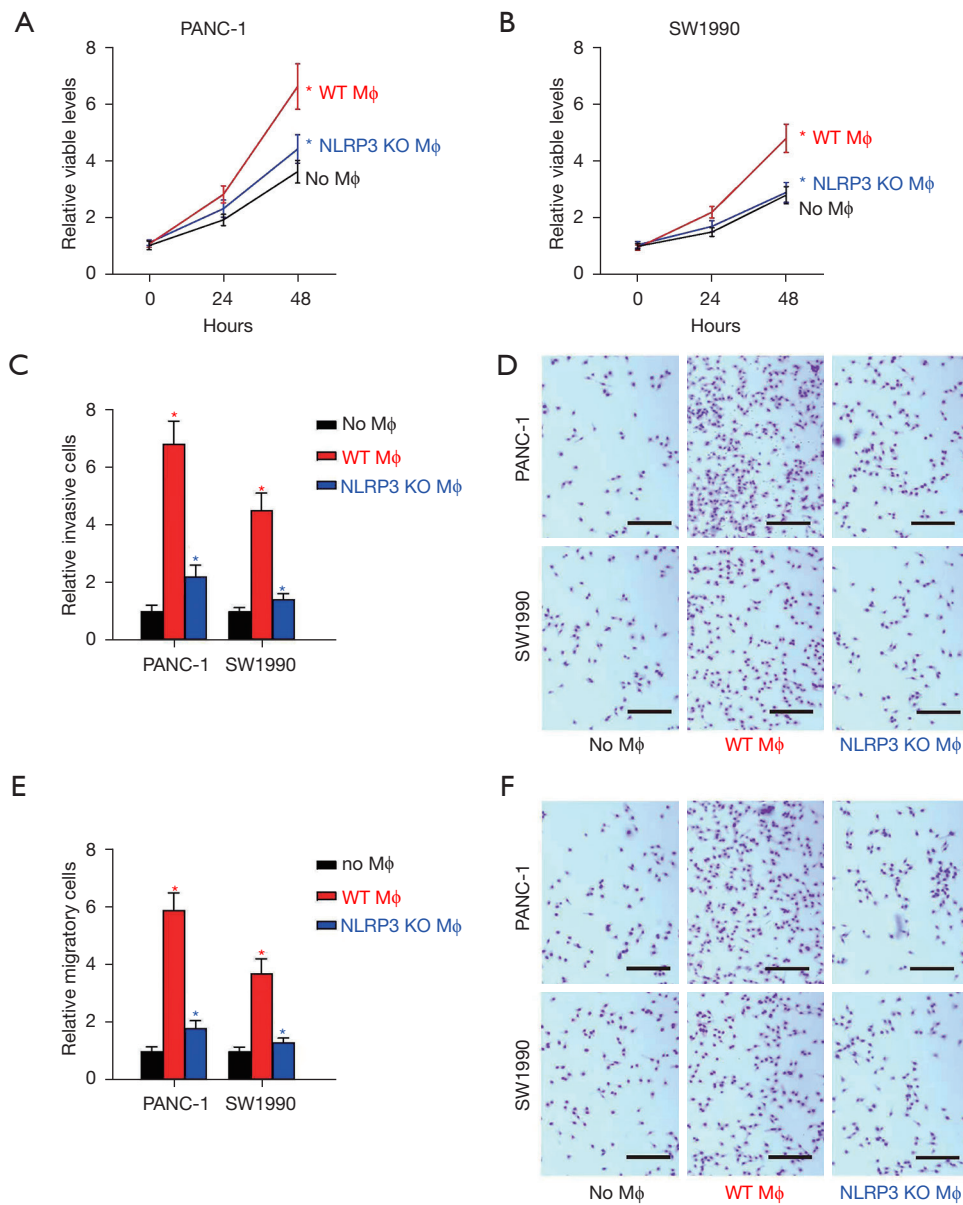
**Figure 3** NLRP3-depletion in macrophages decreases the cell growth, invasion, and migration of cocultured PDAC cells. The regulation of macrophage polarization by NLRP3 was examined in a coculture system by naïve NLRP3 (+/+) or NLRP3 (–/–) macrophages and PDAC cells. (A,B) CCK-8 assay for PANC-1 cells (A) and for SW1990 cells (B). (C,D) Transwell cell invasion assay (the upper chamber was filled with $2 \times 10^5$ PANC-1 cells with macrophages or PANC-1 cells alone), shown by quantification (C) and by representative images stained with 0.1% crystal violet (D). (E,F) Transwell cell migration assay (the upper chamber was filled with $2 \times 10^5$ PANC-1 cells with macrophages or PANC-1 cells alone), shown by quantification (E) and by representative images stained with 0.1% crystal violet (F). *, $P < 0.05$ (red *: WT Mϕ *vs.* no Mϕ; blue *: NLRP3KO Mϕ *vs.* WT Mϕ). N=5. Scale bars were 100 µm. Mϕ: macrophages. WT, wildtype; NLRP3, NLR family pyrin domain containing 3; KO, knockout; PDAC, pancreatic ductal adenocarcinoma; CCK-8, Cell Counting Kit-8.
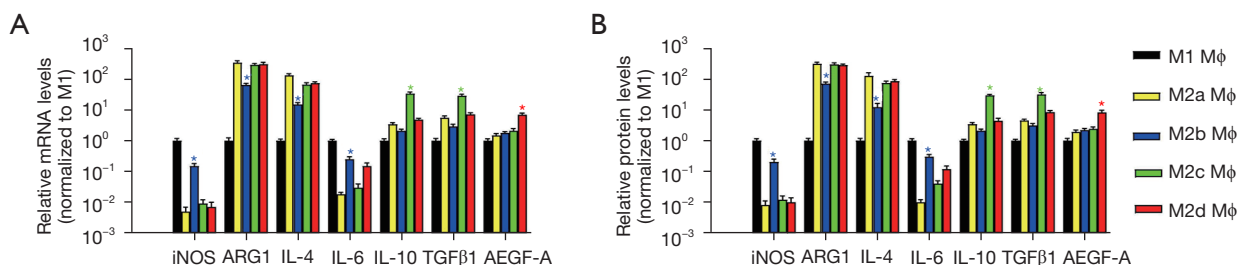
**Figure 4** Differentiation of M1, M2a, M2b, M2c, and M2d macrophages. Naïve macrophages from wildtype mice were differentiated into M1, M2a, M2b, M2c, and M2d macrophages by established methods. (A,B) Expression of polarization markers was analyzed by RT-qPCR (A) and by ELISA (B). *, P<0.05 (red *: M2d *vs.* others; green *: M2c *vs.* others; blue *: M2b *vs.* M2a or M2c or M2d). N=5. Mφ: macrophages. iNOS, inducible nitric oxide synthase; ARG1, arginase 1; IL, interleukin; TGFβ1, transforming growth factor beta 1; VEGF-A, vascular endothelial growth factor A; RT-qPCR, real-time polymerase chain reaction; ELISA, enzyme-linked immunosorbent assay.

M2c, and M2d. The highest levels of IL-10 and TGFβ1 were detected in M2c, while the highest level of VEGF-A was detected in M2d. Together, these data confirmed the successful differentiation of naïve macrophages *in vitro*.

### M1 and M2b macrophages have compromised effects on cell growth, invasion, and migration of cocultured PDAC cells

The effects of differently polarized macrophages on cell growth, invasion, and migration of cocultured PDAC cells were then examined in a coculture system. Cell growth was analyzed using a CCK-8 assay. We found that increases in the number of viable cocultured PANC-1 cells were significantly higher by M2a/M2c/M2d macrophages than M1/M2b macrophages (*Figure 5A*). Cell invasiveness and migratory potential were then analyzed by transwell cell invasion assay and cell migration assay, respectively. We found that the invasiveness of cocultured PANC-1 cells was significantly higher by M2a/M2c/M2d macrophages than M1/M2b macrophages (*Figure 5B,5C*), while the migratory potential of cocultured PANC-1 cells was also significantly higher by M2a/M2c/M2d macrophages than M1/M2b macrophages (*Figure 5D,5E*). Together, these data suggested that M1 and M2b macrophages have compromised effects on the cell growth, invasion, and migration of cocultured PDAC cells.

### NLRP3 depletion inhibits PDAC progression

PDAC formation and progression were analyzed in a mouse model of PDAC with or without NLRP3 knockout.

P48^Cre; LSL-Kras^G12D [KC or KC NLRP3 (+/+)] mice were bred with NLRP3-KO mice to obtain KC NLRP3 (–/–) mice. The KC NLRP3 (+/+) mice were used as controls. We detected NLRP3 in KC NLRP3 (+/+) mice but not in KC NLRP3 (–/–) mice (*Figure 6A*). After 6 months, KC NLRP3 (–/–) mice appeared to have a significantly healthier acinar area than the KC NLRP3 (+/+) mice (*Figure 6B*). Moreover, higher malignant cancer stages were detected in KC NLRP3 (+/+) mice compared with NLRP3 (–/–) mice (*Figure 6C*). Together, these data suggested that NLRP3 depletion inhibited PDAC progression.

### NLRP3 depletion reduces lung metastasis of PDAC

Finally, lung metastasis of the mice was analyzed. Lung metastasis was determined by histology at 6 months. We found that NLRP3 depletion reduced lung metastasis in KC mice from 40% to 10% (*Figure 7A,7B*). These results showed that NLRP3 depletion reduced lung metastasis of PDAC.

### Discussion

PDAC is an aggressive tumor with poor prognosis despite curative surgery. Improving oncologic outcomes of PDAC remains an unmet need that must be fueled by basic science and translational research rather than clinical trials. This study aimed to understand whether targeting TAMs may impact the PDAC initiation, progression, and metastasis (6,14). TAM functions are established when the phenotype of macrophages is determined by the microenvironment mainly regulated by PDAC cells (7). Thus, targeting TAMs
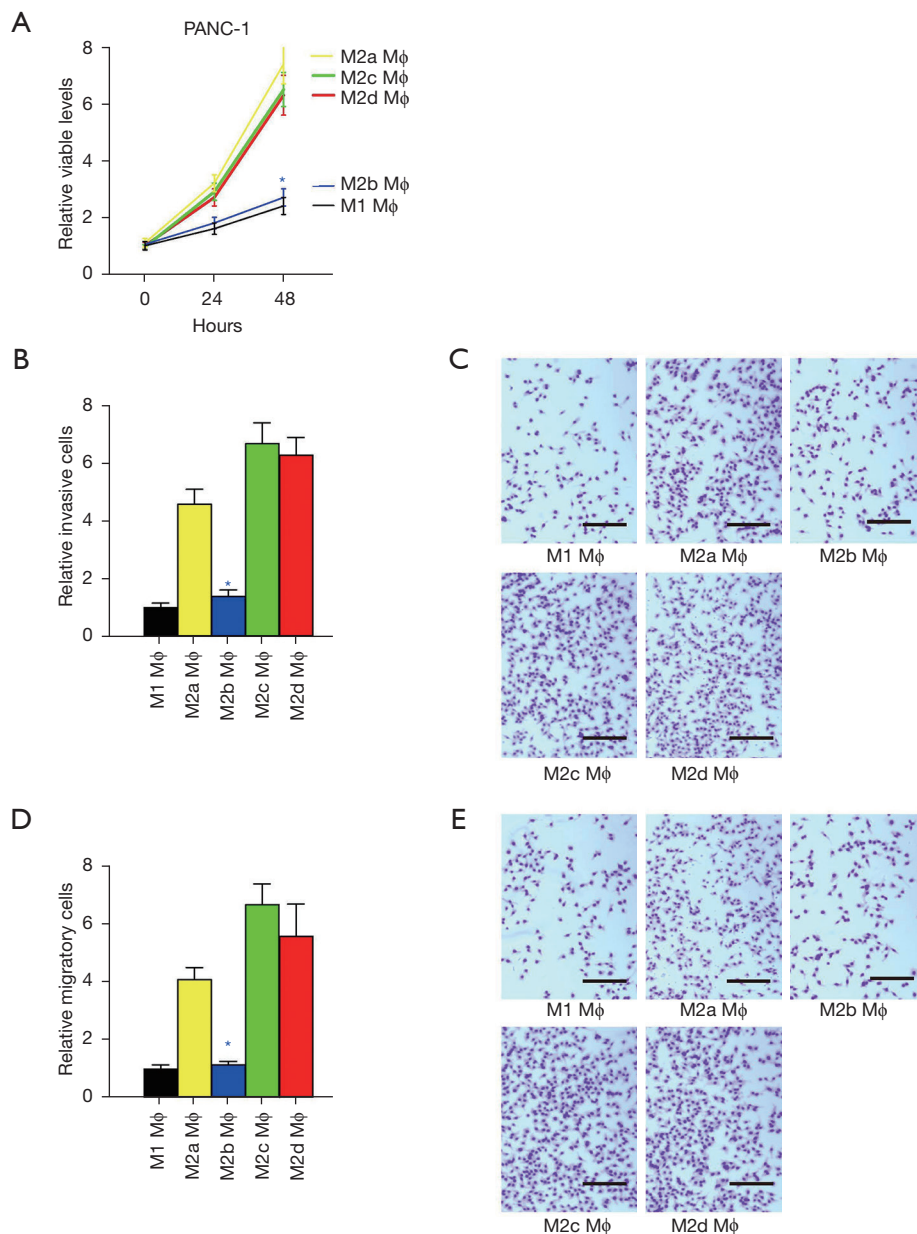
                                

**Figure 5** M1 and M2b macrophages have compromised effects on the cell growth, invasion, and migration of cocultured PDAC cells. The effects of differently polarized macrophages on the cell growth, invasion, and migration of cocultured PDAC cells were examined in a coculture system. (A) CCK-8 assay for PANC-1 cells. (B,C) Transwell cell invasion assay (the upper chamber was filled with $2\times10^5$ PANC-1 cells with differentially polarized macrophages or PANC-1 cells alone), shown by quantification (B) and by representative images stained with 0.1% crystal violet (C). (D,E) Transwell cell migration assay (the upper chamber was filled with $2\times10^5$ PANC-1 cells with differentially polarized macrophages or PANC-1 cells alone), shown by quantification (D) and by representative images stained with 0.1% crystal violet (E). *, $P<0.05$ (blue *: M2b *vs.* M2a or M2c or M2d). N=5. Scale bars were 100 μm. Mϕ: macrophages. PDAC, pancreatic ductal adenocarcinoma; CCK-8, Cell Counting Kit-8.
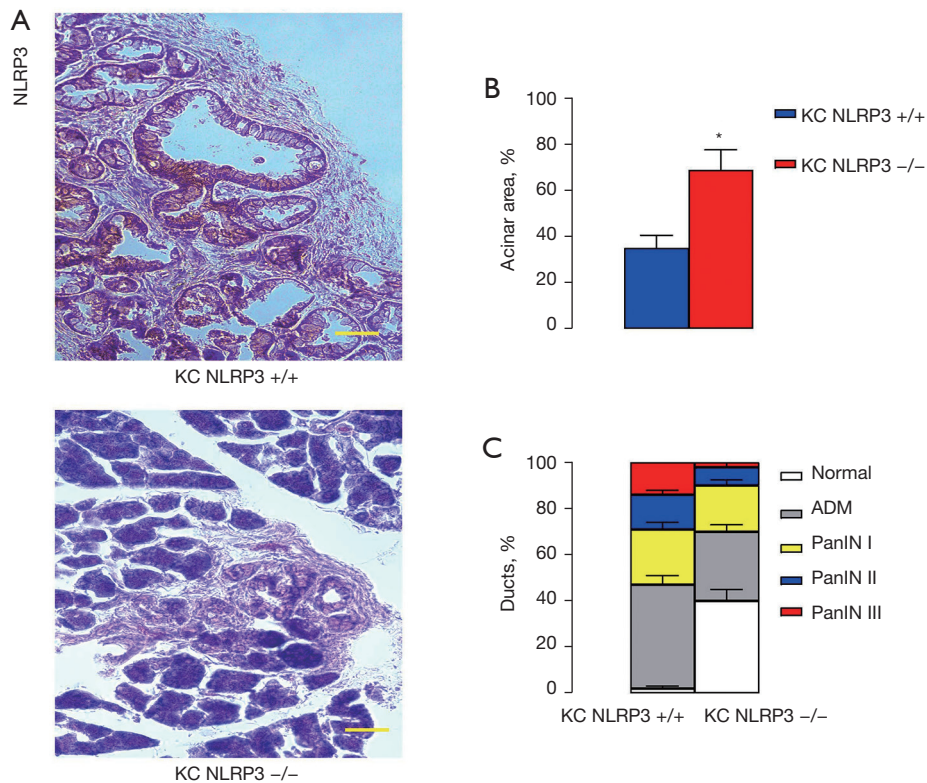
**Figure 6** NLRP3 depletion inhibits PDAC progression. PDAC formation and progression were analyzed in a mouse model of PDAC with or without NLRP3 knockout. P48Cre; LSL-KrasG12D [KC or KC NLRP3 (+/+)] mice were bred with NLRP3-KO mice to obtain KC NLRP3 (−/−) mice. The KC NLRP3 (+/+) mice were used as controls. (A) Representative immunohistochemical images for NLRP3 staining at 6 months. (B,C) Quantification of percentage of healthy acinar area (B) and ducts at different stages (C) at 6 months. N=5. Scale bars were 50 µm. *, P<0.05. NLRP3, NLR family pyrin domain containing 3; KC, LSL-Kras$^{G12D}$; ADM, acinar-to-ductal metaplasia; PDAC, pancreatic ductal adenocarcinoma; KO, knockout; PanIN, pancreatic intraepithelial neoplasia.
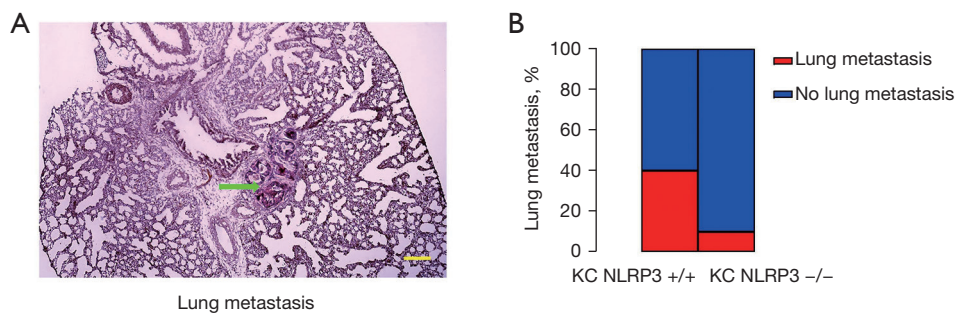


**Figure 7** NLRP3 depletion reduces lung metastasis of PDAC. Lung metastasis was determined by histology at 6 months. (A) A representative histological H&E staining image for lung metastasis (green arrow) of PDAC from a KC NLRP3 +/+ mouse. (B) Quantification of lung metastasis ratio. Scale bar was 200 µm. NLRP3, NLR family pyrin domain containing 3; PDAC, pancreatic ductal adenocarcinoma; KC, LSL-Kras$^{G12D}$; H&E, hematoxylin and eosin.

      

and changing their tumor-supportive characteristics may be an effective strategy for PDAC therapy.

It has been well established that macrophages can be differentiated into either proinflammatory or anti-inflammatory subtypes (15). In the case of cancer, proinflammatory macrophages exhibit anticancer functions, while their polarization to an anti-inflammatory phenotype promotes cancer growth and invasion (16). It has been shown that M2d with M2a and M2c are macrophages that enhance tumor growth and metastasis, while M1 and M2b macrophages have potential to work with other inflammatory cells, such as T cells, to kill cancer cells (17). However, to the best of our knowledge, it is not known whether polarization of TAMs in PDAC is regulated by NLRP3.

Here, we found that *in vitro*, the presence of NLRP3 in macrophages led to M2a/c/d TAM-like polarization when they were cocultured with PDAC cells. Conversely, NLRP3 depletion in macrophages led to M1/M2b polarization when they were cocultured with PDAC cells. NLRP3-depletion in macrophages significantly increased tumor growth and stage progression in a mouse model of PDAC and significantly increased the occurrence of lung metastasis. Since IL-1β and IL-18 are activated by NLRP3 (10), they may be important regulators for macrophage polarization, either directly or indirectly. Interestingly, NLRP3 depletion has been shown to affect tumorigenesis, tumor progression and metastasis in prostate cancer (18), colorectal carcinoma (19), gastric cancer (20) and breast cancer (21).

Although IL-1β is considered as an important proinflammatory cytokine, it is known that macrophage polarization is a complex process involving M1/M2 transit subtypes (22). At the early stage of M2 polarization, IL-1β remains very high (23). Therefore, it is possible that activation of NLRP3/IL-1β signaling cascades may be crucial for finalizing or maintaining an M2a/c/d phenotype, and while NLRP3 is depleted in our experiments, the M2a/c/d differentiation is halted or aborted (23). These hypotheses were not addressed here, as a limitation of the current study. Further investigations will reveal intriguing findings in future studies.

Collectively, our results demonstrated that NLRP3 in TAMs may be an important target for PDAC therapy.

## Acknowledgments

## Footnote

## References

1. De Rosa P, Jewell A. The potential use for patient reported outcome measures in people with pancreatic cancer, with a specific focus on older patients. Eur J Surg Oncol 2021;47:495-502.
2. Ristau P, Oetting-Roß C, Büscher A. Coping in patients with pancreatic cancer: a scoping review and narrative synthesis. BMJ Support Palliat Care 2021. [Epub ahead of print]. doi: 10.1136/bmjspcare-2021-003266.

868

Gu et al. TAM NLRP3 in lung metastasis of PDAC

3. Homma Y, Endo I, Matsuyama R, et al. Outcomes of lung metastasis from pancreatic cancer: A nationwide multicenter analysis. J Hepatobiliary Pancreat Sci 2022. [Epub ahead of print]. doi: 10.1002/jhbp.1127.

4. Sasaki T, Nishiwada S, Nakagawa K, et al. Integrative analysis identifies activated anti-tumor immune microenvironment in lung metastasis of pancreatic cancer. Int J Clin Oncol 2022;27:948-57.

5. Xavier CPR, Castro I, Caires HR, et al. Chitinase 3-like-1 and fibronectin in the cargo of extracellular vesicles shed by human macrophages influence pancreatic cancer cellular response to gemcitabine. Cancer Lett 2021;501:210-23.

6. Geng Y, Fan J, Chen L, et al. A Notch-Dependent Inflammatory Feedback Circuit between Macrophages and Cancer Cells Regulates Pancreatic Cancer Metastasis. Cancer Res 2021;81:64-76.

7. Yang J, Li Y, Sun Z, et al. Macrophages in pancreatic cancer: An immunometabolic perspective. Cancer Lett 2021;498:188-200.

8. Taylor PR, Martinez-Pomares L, Stacey M, et al. Macrophage receptors and immune recognition. Annu Rev Immunol 2005;23:901-44.

9. Carmi Y, Rinott G, Dotan S, et al. Microenvironment-derived IL-1 and IL-17 interact in the control of lung metastasis. J Immunol 2011;186:3462-71.

10. Sharma BR, Kanneganti TD. NLRP3 inflammasome in cancer and metabolic diseases. Nat Immunol 2021;22:550-9.

11. Lin TY, Tsai MC, Tu W, et al. Role of the NLRP3 Inflammasome: Insights Into Cancer Hallmarks. Front Immunol 2021;11:610492.

12. Hingorani SR, Petricoin EF, Maitra A, et al. Preinvasive and invasive ductal pancreatic cancer and its early detection in the mouse. Cancer Cell 2003;4:437-50.

13. Hruban RH, Adsay NV, Albores-Saavedra J, et al. Pancreatic intraepithelial neoplasia: a new nomenclature and classification system for pancreatic duct lesions. Am J Surg Pathol 2001;25:579-86.

14. Tu M, Klein L, Espinet E, et al. TNF-α-producing macrophages determine subtype identity and prognosis via AP1 enhancer reprogramming in pancreatic cancer. Nat Cancer 2021;2:1185-203.

15. Tan Y, Wang M, Zhang Y, et al. Tumor-Associated Macrophages: A Potential Target for Cancer Therapy. Front Oncol 2021;11:693517.

16. Liu J, Geng X, Hou J, et al. New insights into M1/M2 macrophages: key modulators in cancer progression. Cancer Cell Int 2021;21:389.

17. Raskov H, Orhan A, Gaggar S, et al. Cancer-Associated Fibroblasts and Tumor-Associated Macrophages in Cancer and Cancer Immunotherapy. Front Oncol 2021;11:668731.

18. Xu Z, Wang H, Qin Z, et al. NLRP3 inflammasome promoted the malignant progression of prostate cancer via the activation of caspase-1. Cell Death Discov 2021;7:399.

19. Li T, Fu B, Zhang X, et al. Overproduction of Gastrointestinal 5-HT Promotes Colitis-Associated Colorectal Cancer Progression via Enhancing NLRP3 Inflammasome Activation. Cancer Immunol Res 2021;9:1008-23.

20. Zhang X, Li C, Chen D, et al. H. pylori CagA activates the NLRP3 inflammasome to promote gastric cancer cell migration and invasion. Inflamm Res 2022;71:141-55.

21. Yan H, Luo B, Wu X, et al. Cisplatin Induces Pyroptosis via Activation of MEG3/NLRP3/caspase-1/GSDMD Pathway in Triple-Negative Breast Cancer. Int J Biol Sci 2021;17:2606-21.

22. Maruyama K, Nemoto E, Yamada S. Mechanical regulation of macrophage function - cyclic tensile force inhibits NLRP3 inflammasome-dependent IL-1β secretion in murine macrophages. Inflamm Regen 2019;39:3.

23. Pelegrin P, Surprenant A. Dynamics of macrophage polarization reveal new mechanism to inhibit IL-1beta release through pyrophosphates. EMBO J 2009;28:2114-27.

(English Language Editor: A. Muylwyk)